CANADIAN RESEARCH COMBINING NEUTRON REFLECTOMETRY AND ELECTROCHEMISTRY

BY JAMES J. NOËL

Neutron reflectometry (NR) is a powerful technique for probing surface layers, because it is sensitive to isotopic makeup and has excellent depth resolution, typically 0.5-1 nm, for layers in the range 0.5-300 nm thick. It is non-destructive and often amenable to in-situ observations. Its applications are well described [1-3]. Canadian NR capabilities have yielded key data on a variety of experimental systems: polymers [4-10], adsorbed layers [11,12], hydrogen storage materials [13-19], electrochemical capacitors [20], and corroding metals [21-26].

NR is based on specular reflection of neutrons from a planar surface, or from a series of layered interfaces. As does optical reflectivity technique, NR yields information on the differences between the refractive indices of the materials on either side of the interface in the form of a profile in the direction normal to the interface. The neutron refractive index of a material is related to its scattering length density (SLD), the weighted average of ρb of all the material's components, where ρ is the number density of atomic nuclei and b is their coherent neutron scattering length, an intrinsic and isotope-specific property of the atomic nucleus. NR can reveal a compositional depth profile of the interfacial layers to about 1 at.%, and its isotopic sensitivity is useful for isotopic labelling experiments or contrast matching [1]. When the surface contains multiple layers, a portion of the incident coherent neutron beam reflects from each interface, creating an interference pattern at the detector, which is related to the thickness of each of the surface layers by Bragg's law.

THE HISTORY OF NR IN CANADA

The earliest NR experiments [1] were reported in the 1980s, and NR became available in Canada in 1992 at the NRU reactor at Chalk River. The first experiments at NRU were conducted on a system of giant magnetoresistance (GMR) multilayers [27,28], for which beam scientist Zin Tun configured the C5 triple axis neutron spectrometer as a part-time reflectometer, since C5 already had the components required for reflectometry: monochromator; rotatable sample table; neutron detectors for signal counting and beam monitoring (in lieu of a reference beam); collimating slits; computer for instrument control and data acquisition; and radiation shielding (see schematic in Fig. 1). Only high-precision collimating slits had to be added for NR, and further success with studies of magnetism [28], polymer surfaces [7,8], and corrosion [22-26] facilitated formation of a user community that supported the construction of the CFI-funded custom-built neutron reflectometer at the D3 beam (Fig. 2) to improve quality of data and ease of operation. The D3 reflectometer, which was completed in 2007 and described by Fritzsche [10], was designed to balance competing issues, such as functionality, complexity and cost; high neutron flux versus low background; and resolution versus dynamic range [9]. Amongst its optimizations are: a very tall focusing monochromator to maximize neutron flux on the sample, a limiting parameter that determines resolution or time required for data collection; a correspondingly tall 32-wire detector for simultaneous measurement of specular and off-specular reflections; and supermirror polarizers for measurements involving magnetism. It was designed with the capacity to use cold neutrons, so that it could later be relocated to a reactor with a cold neutron source.

SUMMARY

I overview Canadian neutron reflectometry, with a focus on applications in electrochemical and corrosion science research.

SOLID-LIQUID ELECTROCHEMICAL SETUP

Difficulties in passing neutrons through the electrolyte solution, or in obtaining large, flat interfaces in a solid electrolyte cell, make NR challenging for electrochemistry at liquid-liquid or solid-solid interfaces, respectively, but the solid-liquid electrochemical NR setup is often amenable for in-situ NR, even at elevated temperatures and pressures. The solid-liquid case uses some of neutrons' unique properties, including high penetrating power in most solids. They can be directed through the substrate, instead of through hydrogenous solutions, as is often done with electromagnetic probes, because hydrogen has high neutron cross-sections for absorption and inelastic scattering. Typically, a very thin, uniform layer of the electrode material, deposited on a substrate, is mounted in an

James J. Noël,
<jjnoel@uwo.ca>,
Department of Chemistry and Surface Science
Western, The University of Western Ontario,
London, ON N6A 5B7

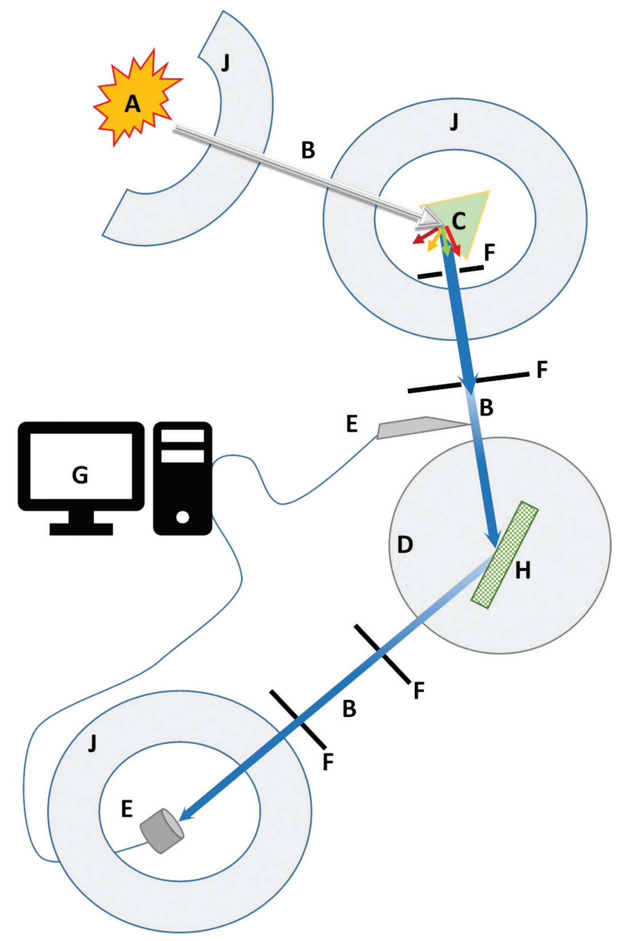

Fig. 1 Schematic layout of a neutron reflectometer, showing: **A**-neutron source; **B**-neutron beam; **C**-monochromator; **D**-rotatable sample table; **E**-neutron detectors for signal counting and beam monitoring (in lieu of reference beam); **F**-collimating slits; **G**-computer for instrument control and data acquisition; **H**-sample; and **J**-massive radiation shielding.

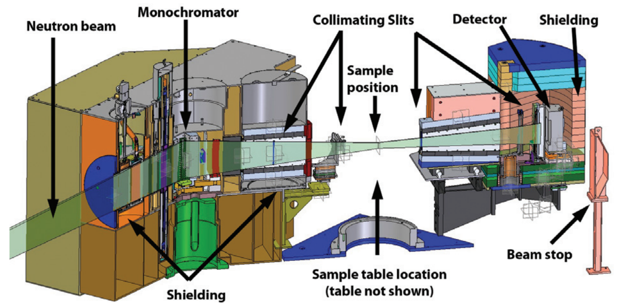

Fig. 2 Cut-away diagram of the D3 reflectometer at Chalk River Laboratories, with key features highlighted.

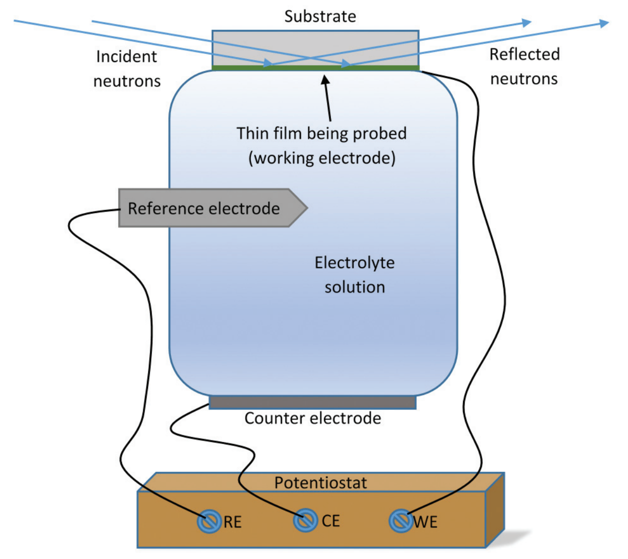

Fig. 3 Schematic illustration of electrochemical setup showing the path of neutrons through the substrate. The substrate, coated with the material under study, may be made to reside at the top, bottom or sidewall of the electrochemical cell, affording flexibility for work at a reflectometer with either vertical or horizontal beam orientation and with systems affected by the gravitational field.

electrochemical cell that allows neutrons to pass through the "back" of the electrode and reflect from the electrode-solution interface, continuing then to travel through the underlying substrate toward the detector (Fig. 3). Only neutrons that have reflected before crossing the outermost layer of the electrode-solution interface are detected. Thus, the electrochemistry in the solution does not interfere with the NR measurement. The surface can be configured either horizontally or vertically to suit the orientation of the reflectometer, but practical considerations, such as removal of evolved gas bubbles, or buoyancy or hydrophilicity effects on adsorbates, may favour one or the other orientation.

NR requires a very large, single-crystal substrate of a neutron-transparent material, such as silicon, quartz, or sapphire, which must be polished nearly atomically flat. Single crystal substrates avoid undesired scattering from grain boundaries. Neutron-transparency is needed since neutrons may travel through the full length of the substrate at the glancing incidence angles (<5°) required for reflection.

Similarly, the deposited electrode layer must also be thin, flat, and uniform over several square centimetres. Thinness minimizes incoherent and inelastic scattering. The large surface area is required for two reasons: (1) the low neutron flux, which is much lower than flux in analogous optical techniques, requires a larger beam, and (2) even with a narrow ribbon-shaped beam, the beam footprint is large at the glancing incidence angles (<5°) required for reflection. That is, there is a wide separation between where the front of the beam hits the interface and the point where the back of the beam encounters it (Fig. 3). Since the maxima and minima in the reflected neutron interference pattern are related via Bragg's law to the thicknesses in a system of layers, flatness and uniformity of the electrode are essential to distinguish layers as thin as 1 nm from the surface roughness. Electrode preparation is not as daunting as it may sound. For example, the author has used 10 cm diameter single-crystal Si slabs of 6 mm thickness as substrates [21-26], with measured intensity losses of only about 15% over the 10 cm path that the neutrons travel through the Si.

CORROSION STUDIES

Much in-situ electrochemical NR research at Chalk River has been on corrosion of metals, particularly Ti [21-26], Zr [25,26], and Zr-2.5Nb alloy [24], because of their importance to the Canadian nuclear industry: Zr and Zr-Nb alloys are used in reactor fuel channels and fuel sheathing, and Ti was a candidate material for fabrication of nuclear fuel waste disposal containers, though it has been displaced for this purpose by copper-coated steel [29]. These metals are well suited for in-situ electrochemistry NR experiments, first, because they can be prepared by magnetron sputtering deposition. Second, their spontaneously-formed passive oxide films exhibit no roughening due to localized corrosion and they have very low corrosion rates, which enables stability over the 8-24 h periods required to collect clean, low noise NR data. Third, they tend to absorb atomic hydrogen, a common by-product of corrosion, and in situ NR has a rare ability to quantify hydrogen in metals non-destructively. Thus, we could simultaneously measure the metal and oxide layer thickness and composition, including hydrogen content, observing oxide film growth or hydrogen absorption as a function of electrochemical potential.

Titanium

On Ti, NR revealed that the air-formed passive oxide was a single layer with composition and density corresponding to that of the rutile polymorph. Neither the oxide layer nor the underlying metal changed when exposed to deaerated, near-neutral pH aqueous NaCl at the open-circuit potential [22,23]. However, applying anodic polarization thickened the oxide layer at the expense of the metal layer, and the metal absorbed a small amount of oxygen. The anodization ratio (potential-driven thickening), Pilling-Bedworth (volume expansion) ratio, and ionic transport numbers determined by NR were consistent with reported values determined by other means. Unlike the air-formed oxide, the anodic oxide consisted of two layers, an inner "dry" TiO_2 and an outer hydrated oxide with high OH content. Subsequent cathodic polarization changed the composition, but not the thickness of the oxide film. At more negative potentials, the film absorbed hydrogen progressively from the outer surface, increasing the outer hydrated oxide region's hydrogen content, converting the "dry" inner oxide (possibly reducing it to TiO(OH)), and penetrating into the underlying Ti metal. At a potential of −1.4 V vs the saturated calomel electrode (SCE), the inner "dry" oxide appeared to be almost fully hydrogenated, and at the next step of the polarization, −1.6 V(SCE), the electrode was destroyed by rapid hydrogen ingress into the metal and formation of gaseous hydrogen bubbles at the Si/Ti interface. Blisters and tattered remnants of burst metallic bubbles were visible on the electrode surface after the experiment [22,23].

More detailed studies to determine a threshold potential for hydrogen entry into Ti [21] were conducted in heavy water (D_2O) to create a higher contrast when hydrogen is absorbed in Ti. While natural abundance Ti and ^1H have negative SLD, deuterium's SLD is positive. Electrochemical impedance spectroscopy (EIS) measurements were made simultaneously with NR to link hydrogen absorption with changes in the oxide film's electronic properties. This approach allowed us to reconcile conflicting reports of the threshold potential for hydrogen entry into Ti: −0.37 V(SCE) and −0.6 V(SCE). At –0.37 V(SCE), significant changes in current density, oxide resistivity and capacitance, and the SLD of the Ti indicated the onset of oxide conductivity, D atom adsorption, and D ingress through electronically conductive, physically defective pathways in the oxide. At −0.6 V(SCE), both the current density and the D content in the Ti film increased substantially, and this potential was recognized as the threshold for reducing the protective oxide from the original TiO_2 to a less-protective TiOOD (i.e., TiOOH) and rendering it ineffective as a barrier to hydrogen ingress.

Zirconium and Zr-2.5Nb Alloy

On Zr in near-neutral Na_2SO_4 solution, the anodization ratio determined using NR was 3.4 nm·V^{-1}, somewhat higher than the generally accepted anodization ratio for Zr (2.8 nm·V^{-1}) determined by coulometry. The Pilling-Bedworth ratio was in good agreement with the value calculated from bulk densities or crystal lattice parameters [25,26]. Surprisingly, the oxide film growth continued beyond the expected logarithmic growth, albeit at a very low rate, for upwards of 12 h. EIS detected cracking in the oxide film at potentials above 1 V(SCE) when its thickness exceeded ~12 nm, evident in the sudden decrease of oxide film resistance and loss of passivation. Water in the cracks lowered the oxide layer SLD, and corrosion at the base of the cracks resulted in hydrogen absorption in the metallic Zr layer, a surprising observation, as cathodic polarization is normally required for hydrogen absorption. Neither the anodization ratio nor the Pilling-Bedworth ratio showed any discontinuity at the time of oxide cracking, and the EIS retained its single time constant response. These observations were taken as evidence that the cracks and intact regions of the electrode were behaving nearly independently, as parallel electrodes. In situ EIS measurements [26] were used to determine the oxide film capacitance and resistance. Since NR provided an independent measure of the oxide layer thickness, it was possible to calculate the dc dielectric constant and resistivity of the oxide film according to $\varepsilon = Cd/A\,\varepsilon°$, where ε isthe dc dielectric constant, C the capacitance, d the oxide film thickness, A the surface area, and $\varepsilon°$ the permittivity of free space, and to $r = RA/d$, where r is resistivity, and R resistance. The dc dielectric constant was at the lower end of the range of published values (25-56), and remained constant over the potential range −0.17 V(SCE) to 3 V(SCE), showing no deviation when the oxide film cracked. The resistivity was constant over the polarization range from −0.17 V(SCE) to 1 V(SCE) up to the point of oxide cracking.

Under cathodic polarization, NR showed that no hydrogen absorption into either the oxide or the metal, nor layer thickness changes, occurred, down to a potential of −2.5 V(SCE) [25,26]. EIS, however, detected significant changes. Immediately after the polarity reversal from 3 V(SCE) to −1 V(SCE), the oxide film resistance increased by more than an order of magnitude, due to repassivation of the metal at the base of the cracks in the oxide (not detected by NR due to small surface coverage by cracks). As the potential was decreased stepwise to −3 V(SCE), both the resistance and capacitance of the oxide layer decreased because of increased conductivity due to band bending in the semiconducting oxide (wide bandgap = 5.7 V) and possibly hydrogen doping at levels too low to detect by NR (i.e., <1 at.%).

The alloy Zr-2.5Nb, which is used to fabricate pressure tubes in CANDU® reactors, behaved much like pure Zr in that the oxide film thickened anodically and cracked at potentials above 1 V(SCE), with water filling the cracks, leading to hydrogen absorption into the underlying alloy [24]. The Pilling-Bedworth ratio was very similar to that of the pure Zr, but the anodization ratio was different, assuming two values, $1.74\ \mathrm{nm{\cdot}V^{-1}}$ between –0.2 and 0.7 V(SCE) and $4.85\ \mathrm{nm{\cdot}V^{-1}}$ between 0.7 and 2.0 V(SCE). Under cathodic polarization, NR observed no changes to either the oxide layer or the underlying metal, just as for pure Zr.

Co_3O_4

The spinel-structure oxide Co_3O_4 is a redox-active semiconductor material (bandgap ~1.1 V) that is of interest for supercapacitor applications, due to its large electrochemical pseudocapacitance. In situ NR using contrast-matched mixtures of H_2O and D_2O, combined with EIS, was used to probe the extent and reversibility of chemical changes occurring during activation of its pseudocapacitative properties [20]. Immersed in water, the oxide layer swelled from 44 nm to 54 nm thick and about 40% converted to CoOOH, distributed uniformly through the layer. Increasing the pH changed the open circuit potential and the EIS response, due to chemical or electronic property changes in a very thin layer, below detection by NR, at the oxide-substrate interface. Anodic polarization to 1 V(SCE) resulted in further conversion of the oxide to CoOOH (65%), which spontaneously reversed after the anodic polarization was removed.

ADSORPTION-DESORPTION OF SURFACTANT MOLECULES AT THE METAL-AQUEOUS SOLUTION INTERFACE

The final electrochemistry-NR experiments summarized here were performed by Canadians in collaboration with instrument scientists on the NG-7 reflectometer at the NIST Center for Neutron Research (USA), because NG-7 operates in the horizontal configuration, an orientation not available in Canada. The horizontal configuration was important to control for gravitational effects such as buoyancy and preference of surfactant molecules for the air-solution interface. In these experiments, a thin film of gold, deposited onto a quartz substrate with a chromium adhesion layer on its surface, was used as the electrode, and the electrochemical potential-driven adsorption and desorption of a surfactant was monitored simultaneously by electrochemical and NR methods. The surfactants studied included mixtures of dimyristoylphosphatidylcholine (DMPC) with cholesterol [30,31], 4-Pentadecyl-pyridine (C15-4Py) [32,33], n-octadecanol [34], sodium dodecyl sulfate (SDS) [35-37], N-dodecyl-N,N-dimethyl-3-ammonio-1-propanesulfonate (DDAPS) [36], and N-decyl-N,N,N-trimethylammonium triflate (DeTATf) [36].

By controlling the potential, the charge density at the metal surface can be varied from about $-30\ \mu C/cm^2$ to about $40\ \mu C/cm^2$, which, over the very short distances relevant to the electric double layer at the electrode-electrolyte interface, generates fields on the order of 10^{10} V/m. Such a field strongly influences the energetics of interactions between the metal surface and polar molecules at the interface [35]. Because the field can be varied enormously, surfactant molecules can be made to adsorb, desorb, or change orientation during NR. The authors used NR to monitor the thickness and density of surfactant layers under controlled conditions and, by employing H_2O-D_2O mixtures in the electrolyte solution, determine the water content of the surfactant films. Together with independently obtained spectroscopic information from techniques like polarization modulation infrared reflection-absorption spectroscopy (PM-IRRAS), NR measurements allowed them to determine: the surfactant layer thickness; whether they had formed monolayer or bilayer films; the orientation of the molecules on the surface; and the amount of water incorporated into or under the films. They found that the electrochemical potential-driven desorption process sometimes led to formation of partially desorbed hemi-micelle structures with water trapped between gold and surfactant aggregates, or individual micelles [31-37].

FUTURE DIRECTIONS

With the permanent shutdown and decommissioning of Chalk River’s NRU reactor, Canadian scientists will have to rely on access to foreign neutron laboratories for performing their NR experiments, at least in the short term. Reflectometers, each with unique capabilities, are available at NIST Centre for Neutron Research (USA), Oak Ridge National Laboratory (USA), the Institut Laue Langevin (France), the OPAL Reactor (Australia), the ISIS Neutron and Muon Source (UK) and others. In the medium term, a reflectometer could be made to function at the McMaster Nuclear Reactor in Hamilton, ON. Two reflectometers are planned at the extremely intense European Spallation Source, which is under construction and is expected to have its first beamlines available to users in 2023. In the long term, the only satisfactory outcome will be for Canada to construct its own domestic neutron source.

Future improvements in NR experiments will come from new, higher flux sources that offer better resolution for a given experiment time or quicker experiments for a given resolution. NR is limited by the need for very large samples (normally several cm in at least one direction) due to the compromise between the neutron flux and the beam footprint geometry. Higher flux will enable NR on some materials that are now very difficult or impossible for NR.

Improvements to record and thoroughly analyze off-specular and grazing incidence scattering to probe in-plane structures and correlation phenomena are under development. The D3 reflectometer, with its 32-wire detector for simultaneous capture of specular and off-specular reflectivity, represents initial progress.

Time-resolved NR to capture system kinetics is an exciting new area. Until recently, most NR experiments have examined systems at steady-state or those with very slow kinetics to compensate for the very long data acquisition times. Time-resolved NR is now being put into practice by time-stamping every neutron count at the detector to deconvolute the spatial and compositional information from its time dependence [38-40].

Another promising area is in coupling NR with other analytical techniques, such as spectroscopic and scanning probe methods that add other simultaneous dimensions of exploration; e.g., in the X-Y plane or in chemical reactivity or composition, including EIS, as described in this paper, and FTIR.

Undoubtedly, NR will prove to be at its greatest advantage when employed in combination with one or more other advanced methods.

REFERENCES

1. J. Penfold and R.K. Thomas, “The application of the specular reflection of neutrons to the study of surfaces and interfaces”, *J. Phys. Condensed Matter*. **2**, 1369-1412 (1990).
2. *Neutron Reflectometry: A Probe for Materials Surfaces*, Proceedings of a Technical Meeting, Vienna, August 16–20, 2004, International Atomic Energy Agency, Vienna, STI/PUB/1246 (2006), 198 pp.
3. H. Fritzsche, “Neutron Reflectometry” in Characterization of Materials, E.N. Kaufmann (*Editor*), John Wiley & Sons (2012), pp. 2226-2237.
4. L.D. Unsworth, Z. Tun, H. Sheardown, and J.L. Brash, “In situ neutron reflectometry investigation of gold-chemisorbed PEO layers of varying chain density: Relationship of layer structure to protein resistance”, *J. Colloid and Interface Sci*. **296**, 520-526 (2006).
5. W.P. Kalisvaart, H. Fritzsche, and W. Mérida, “Water uptake and swelling hysteresis in a nafion thin film measured with neutron reflectometry”, Langmuir, **31**, 5416-5422 (2015).
6. O.M. Tanchak, K.G. Yager, H. Fritzsche, T. Harroun, J. Katsaras, and C.J. Barrett, “Ion distribution in multilayers of weak polyelectrolytes: A neutron reflectometry study”, *J. Chem. Phys*. **129**, 084901 (1-10) (2008).
7. W. Feng, M.-P. Nieh, S. Zhu, T.A. Harroun, J. Katsaras, and J.L. Brash, “Characterization of protein resistant, grafted methacrylate polymer layers bearing oligo(ethylene glycol) and phosphorylcholine side chains by neutron reflectometry”, *Biointerphases*, **2**, 34-43 (2007).
8. L.D. Unsworth, Z. Tun, H. Sheardown, and J.L. Brash, “Chemisorption of thiolated poly(ethylene oxide) to gold: surface chain densities measured by ellipsometry and neutron reflectometry”, *J. Colloid Interface Sci*. **281**, 112-121 (2005).
9. Z. Tun, “Design of a neutron reflectometer at a research reactor”, in *Neutron Reflectometry: A Probe for Materials Surfaces*, Proceedings of a Technical Meeting, Vienna, August 16–20, 2004, International Atomic Energy Agency, Vienna, STI/PUB/1246 (2006) pp. 59-67.
10. H. Fritzsche, “Neutron Reflectometry”, in *Characterization of Materials*, 2nd ed., E.N. Kaufmann (*Editor*), Wiley & Sons (2012) p. 2226.
11. N.M. Pawlowska, H. Fritzsche, C. Blaszykowski, S. Sheikh, M. Vezvaie, and M. Thompson, “Probing the hydration of ultrathin antifouling organosilane adlayers using neutron reflectometry”, *Langmuir*, **30**, 1199-1203 (2014).
12. N.M. Pawlowska, *Probing the hydration of ultrathin antifouling adlayers using neutron reflectometry*, M.Sc. Thesis, University of Toronto, 2014.
13. M. Saoudi, H. Fritzsche, G.J. Nieuwenhuys, and M.B.S. Hesselberth, “Size effect in the spin glass magnetization of thin AuFe films as studied by polarized neutron reflectometry”, *Phys. Rev. Lett*. **100**, 057204 (1-4) (2008).
14. D.L. Cortie, K.-W. Lin, C. Shueh, H.-F. Hsu, X. L. Wang, M. James, H. Fritzsche, S. Brück, and F. Klose, “Exchange bias in a nanocrystalline hematite/permalloy thin film investigated with polarized neutron reflectometry”, *Phys. Rev. B*, **86**, 054408 (1-10) (2012).

15. J. Hoppler, H. Fritzsche, V. K. Malik, J. Stahn, G. Cristiani, H.-U. Habermeier, M. Rössle, J. Honolka, A. Enders, and C. Bernhard, “Polarized neutron reflectometry study of the magnetization reversal process in YBa2Cu3O7/La2/3Ca1/3MnO3 superlattices grown on SrTiO3 substrates”, *Phys. Rev. B*, **82**, 174439 (1-9) (2010).
16. C. Bellouard, C. Tiusan, F. Montaigne, M. Hehn, V. Leiner, H. Fritzsche, and M. Gierlings, “Interlayer magnetic coupling in Fe/MgO junctions characterized by vector magnetization measurements combined with polarized neutron reflectometry”, *Phys. Rev. B*, **78**, 134429 (1-6) (2008).
17. L. Cheng, Z. Altounian, D.H. Ryan, J.O. Ström-Olsen, M. Sutton, and Z. Tun, “Pd polarization and interfacial moments in Pd-Fe multilayers”, *Phys. Rev. B*, **69**, 144403 (1-5) (2004).
18. H. Fritzsche, M. Saoudi, K. Temst, and C. Van Haesendonck, “A polarized neutron reflectometry study of the spin glass freezing in a 29 nm thick AuFe film”, *Physica B*, **397**, 47-49 (2007).
19. H. Fritzsche, M. Saoudi, J. Haagsma, C. Ophus, E. Luber, C.T. Harrower, and D. Mitlin, “Neutron reflectometry study of hydrogen desorption in destabilized MgAl alloy thin films.” *Appl. Phys. Lett.* **92**, 121917 (2008).
20. M. Vezvaie, P. Kalisvaart, H. Fritzsche, Z. Tun, and D. Mitlin, “The penetration depth of chemical reactions in a thin-film Co3O4 supercapacitor electrode”, *J. Electrochem. Soc.* **161**, A798-A802 (2014).
21. M. Vezvaie, J.J. Noël, Z. Tun, and D.W. Shoesmith, “Hydrogen absorption into titanium under cathodic polarization: An in-situ neutron reflectometry and EIS study”, *J. Electrochem. Soc.* **160**, C414-C422 (2013).
22. Z. Tun, J.J. Noël, and D.W. Shoesmith, “Electrochemical modifications on the surface of a Ti film”, *Physica B*, **241-243**, 1107-1109 (1998).
23. Z. Tun, J.J. Noël, and D.W. Shoesmith, “Electrochemical modification of the passive oxide layer on a Ti film observed by in situ neutron reflectometry”, *J. Electrochem. Soc.* **146**, 988-994 (1999).
24. J.J. Noël, H.L. Jensen, Z. Tun, and D.W. Shoesmith, “Electrochemical modification of the passive oxide layer on Zr-2.5Nb observed by in situ neutron reflectometry”, *Electrochemical and Solid-State Letters*, **3**, 473-476 (2000).
25. Z. Tun, J.J. Noël, and D.W. Shoesmith, “Anodic oxide growth on Zr in neutral aqueous solution”, *Pramana J. Phys.* **71**, 769-776 (2008).
26. J.J. Noël, D.W. Shoesmith, and Z. Tun, “Anodic oxide growth and hydrogen absorption on Zr in neutral aqueous solution: A comparison to Ti”, *J. Electrochem. Soc.* **155**, C444-C454 (2008).
27. Z. Tun, “Development of neutron reflectometry in Canada (or the breaking of the chicken-and-egg conundrum)”, *Neutron News*, **14**, 33-35 (2003).
28. Z. Tun, W.J.L. Buyers, I.P. Swainson, M. Sutton, and R.W. Cochrane, “Magnetic order and spin-flop transition in Co-Be multilayers”, *J. Appl. Phys.* **76**, 7075-7077 (1994).
29. D. Heimlich, *APM 2016 lifecycle cost estimate update summary report*, Nuclear Waste Management Organization, Toronto, Report, APM-REP-00440-0202 (2016).
30. I. Burgess, M. Li, S.L. Horswell, G. Szymanski, J. Lipkowski, J. Majewski, and S. Satija, “Electric field-driven transformations of a supported model biological membrane—An electrochemical and neutron reflectivity study”, *Biophysical J.* **86**, 1763-1776 (2004).
31. I. Burgess, M. Li, S.L. Horswell, G. Szymanski, J. Lipkowski, S. Satija, and J. Majewski, “Influence of the electric field on a biomimetic film supported on a gold electrode”, *Colloids and Surfaces B: Biointerfaces*, **40**, 117-122 (2005).
32. V. Zamlynny, I. Burgess, G. Szymanski, J. Lipkowski, J. Majewski, G. Smith, S. Satija, and R. Ivkov, “Electrochemical and neutron reflectivity studies of spontaneously formed amphiphilic surfactant bilayers at the gold-solution interface”, *Langmuir*, **16**, 9861-9870 (2000).
33. I. Burgess, V. Zamlynny, G. Szymanski, A.L. Schwan, R.J. Faragher, J. Lipkowski, J. Majewski, and S. Satija, “Neutron reflectivity studies of field driven transformations in a monolayer of 4-pentadecyl pyridine at Au electrode surfaces”, *J. Electroanal. Chem.* **550-551**, 187-199 (2003).
34. I. Zawisza, I. Burgess, G. Szymanski, J. Lipkowski, J. Majewski, and S. Satija, “Electrochemical, neutron reflectivity and in situ PM-FT-IRRAS studies of a monolayer of n-octadecanol at a Au(111) electrode surface”, *Electrochim. Acta*, **49**, 3651-3664 (2004).
35. J. Majewski, G.S. Smith, I. Burgess, V. Zamlynny, G. Szymanski, J. Lipkowski, and S. Satija, “Neutron reflectivity studies of electric field driven structural transformations of surfactants”, *Appl. Phys. A*, **74**, S364-S367 (2002).
36. M. Chen, I. Burgess, and J. Lipkowski, “Potential controlled surface aggregation of surfactants at electrode surfaces – A molecular view”, *Surf. Sci.* **603**, 1878-1891 (2009).
37. I. Burgess, V. Zamlynny, G. Szymanski, J. Lipkowski, J. Majewski, G. Smith, S. Satija, and R. Ivkov, “Electrochemical and neutron reflectivity characterization of dodecyl sulfate adsorption and aggregation at the gold-water interface”, *Langmuir*, **17**, 3355-3367 (2001).
38. R. Hillman, R. Sapstead, K. Ryder, V. Ferreira, A. Ballantyne, N.-J. Steinke, R. Dalgliesh, *et al.*, “Determination of solvation populations and dynamics in electroactive polymer films by modelling time-resolved neutron reflectivity”, *in Meeting Abstracts*, *The Electrochemical Society*, **45**, 2192-2192 (2016).
39. D. Kawaguchi, A. Nelson, Y. Masubuchi, J.P. Majewski, N. Torikai, N.L. Yamada, A.R.S. Sarah, A. Takano, and Y. Matsushita, “Precise analyses of short-time relaxation at asymmetric polystyrene interface in terms of molecular weight by time-resolved neutron reflectivity measurements”, *Macromolecules,* **44**, 9424-9433 (2011).
40. A.J Clulow, C. Tao, K.H. Lee, M. Velusamy, J.A. McEwan, P.E. Shaw, N.L. Yamada, M. James, P.L. Burn, I.R. Gentle, and P. Meredith, “Time-resolved neutron reflectometry and photovoltaic device studies on sequentially deposited PCDTBT-fullerene layers”, *Langmuir*, **30**, 11474-11484 (2014).